Fluence, flux, and implantation temperature dependence of ion-implantation-induced defect production in 4H–SiC

J. Slotte, K. Saarinen, M. S. Janson, A. Hallén, A. Yu. Kuznetsov, B. G. Svensson, J. Wong-Leung, and C. Jagadish

Fluence, flux, and implantation temperature dependence of ion-implantation-induced defect production in 4H–SiC

J. Slotte[a)] and K. Saarinen
Laboratory of Physics, Helsinki University of Technology, P.O. Box 1100, FIN-02015 HUT, Finland

M. S. Janson[b)] and A. Hallén
*Department of Electronics, Royal Institute of Technology, Electrum 229 SE-164 40,
Kista-Stockholm, Sweden*

A. Yu. Kuznetsov and B. G. Svensson
Department of Physics, University of Oslo, P.O. Box 1048, Blindern, N-0316 Oslo, Norway

J. Wong-Leung and C. Jagadish
*Department of Electronic Materials Engineering, Research School of Physical Sciences and Engineering,
Australian National University, Canberra, ACT 0200, Australia*

Vacancy-type defect production in Al- and Si-implanted 4H–SiC has been studied as a function of ion fluence, ion flux, and implantation temperature in the projected ion range region by positron annihilation spectroscopy and Rutherford backscattering techniques. Ion channeling measurements show that the concentration of displaced silicon atoms increases rapidly with increasing ion fluence. In the ion fluence interval of 10^{13}–10^{14} cm^{-2} the positron annihilation parameters are roughly constant at a defect level tentatively associated with the divacancy $V_C V_{Si}$. Above the ion fluence of 10^{14} cm^{-2} larger vacancy clusters are formed. For implantations as a function of ion flux (cm^{-2} s^{-1}), ion channeling and positron annihilation measurements behave similarly, i.e., indicating increasing damage in the projected range region with increasing ion flux. However, for samples implanted at different temperatures the positron annihilation parameter S shows a clear minimum at approximately 100 °C, whereas the normalized backscattering yield decrease continuously with increasing implantation temperature. This is explained by the formation of larger vacancy clusters when the implantation temperature is increased. © *2005 American Institute of Physics*.
[DOI: 10.1063/1.1844618]

I. INTRODUCTION

Silicon carbide has gained a wide range of interest in the last decade, especially due to its versatility as a base for semiconductor devices working under extreme conditions. SiC has superior material properties which make it suitable for, e.g., high-power devices and high-temperature, high-frequency applications. In order to produce well-defined doped regions in semiconductors, the ion-implantation technique is often used. In the case of SiC, Al implantation has been studied as a possible way of producing p^+-doped regions.[1–3] An obvious disadvantage of the implantation technique is the formation of implantation-induced defects such as vacancies and interstitials. If the fluences are high enough also vacancy clusters and more extended defects can be formed. These defects can hamper the desired electrical properties and therefore thermal annealing of the implanted samples is required in order to reduce the defect density and position dopants at proper substitutional sites. The annealings in SiC often have to be made at very high temperatures[4] since the activation energies for diffusion of intrinsic point defects and dopant atoms in SiC are very high.[5,6] If the im-

plantation damage is too severe the electrical properties of the crystal cannot be restored.[7] In order to reduce the implantation damage and allow point defects to recombine, the implantation can be performed at elevated temperatures,[8] or alternatively the the ion flux can be varied.[9,10]

Positron annihilation spectroscopy (PAS) has previously been used to identify and characterize vacancy-type point defects in semiconductors.[11,12] PAS has been used to identify the two monovacancy species in electron- and proton-irradiated SiC.[13,14] A few PAS studies have been performed on the fluence dependence of the damage production in RT ion-implanted SiC. Brauer *et al.*[15] studied damage production in 200-keV RT Ge-implanted 6H–SiC in the fluence range of 10^{12}–10^{15} cm^{-2}. The main defect in the implanted samples was suggested to be the divacancy. In the amorphous layer created near the surface in the samples implanted with fluences over 3×10^{13} cm^{-2} also bigger vacancy clusters were observed. A number of annealing studies on ion-implanted SiC have been made. Girka *et al.*[16] reported on Xe-implanted and neutron-irradiated 6H–SiC. In their study a "negative" annealing stage, with increasing average lifetime, was observed at 1000 °C. This was attributed to vacancy clustering. Annealing properties of N$_2$- and Al-implanted 3C–SiC were studied by Uedono *et al.*[17] Agglomeration of vacancy-type defects was observed at 20–1000 °C. For annealings at 1000–1200 °C the forma-

[a)]Author to whom correspondence should be addressed; FAX: +358 9 451 3116; electronic mail: jonatan.slotte@hut.fi
[b)]Present address: Institut für Angewandte Physik, Universität Hamburg, Jungiusstrasse 11, D-20355 Hamburg, Germany.

tion of extended defects was seen. These defects annealed out above 1200 °C. A somewhat similar annealing behavior was observed in another study by Uedono *et al.*[18] regarding P-implanted (1×10^{13} cm^{-2}) 6H–SiC. The recrystallization of P implantation (1×10^{15} cm^{-2}) that caused amorphization in 6H–SiC was studied in Ref. 19. Brauer *et al.*[20] noted that the annealing at 500 and 950 °C of 200-keV Ge-implanted 6H–SiC reduced the damaged layer thickness. An annealing temperature of 1500 °C was not enough to remove the vacancy-type defects.

Studies on defect formation in SiC implanted at elevated temperatures can also be found in the literature. Uedono *et al.* studied 3C–SiC implanted at RT to 1200 °C with 200-keV N_2 and Al. They found that at implantation temperatures above 800 °C the main defects trapping positrons were vacancy clusters. Also a shift in the depth distribution of defects toward the surface was observed at higher implantation temperatures. Similar results for 3C–SiC were observed by Itoh *et al.*[21]

Wirth *et al.*[22] combined PAS with Rutherford backscattering spectroscopy (RBS)/channeling to study ion-implantation-induced damage in 6H–SiC. This approach is also applied in the present study, since RBS/channeling monitors dislocated atoms that block the path of a probing ion and thus complements the information of vacancies obtained from the PAS investigations. Ion-implantation damage in SiC has also been extensively studied using only RBS/channeling. Early work by McHargue and Williams[23] and others have been further refined over the last decade and now a fairly broad understanding of the damage accumulation and amorphization exists. The influence of ion fluence, mass, and implantation temperature has been addressed,[4,24,25] and recently also the influence of ion flux[9,26] has been investigated. The Si sublattice is most readily studied by RBS/channeling, but also damage in the C sublattice can be analyzed using nuclear resonance spectroscopy.[27] It is, however, difficult to yield information of specific defects from RBS/channeling and therefore it is very useful to combine this technique with PAS, which is able to provide an identification of vacancy-related defects. For instance, in a previous study we have shown that the formation of defects well below (~ 1 μm) the projected range region of 100-keV Al implants is due to channeled ions and that these defects are mainly V_{Si}.[28]

In practice, when fabricating devices, the implantation of dopants is usually done at a given target temperature and the effect of the ion flux, as an important implantation parameter, is neglected. In this study we use positron annihilation spectroscopy in combination with ion-beam techniques to study the effect of the implantation parameters of ion fluence, ion flux, and implantation temperature on the damage production in the projected ion range region.

II. EXPERIMENTAL TECHNIQUES AND SAMPLE PREPARATION

A. Samples

Three sets of samples were fabricated, the first set was implanted with 100-keV Al ions, with the fluence varying between 10^{12} and 10^{15} cm^{-2}. The second set was used to

TABLE I. Summary of samples used in the study.

Ion	Implantation energy (keV)	Fluence (cm^{-2})	Flux (cm^{-2} s^{-1})	Implantation temperature (°C)
Al	100	1×10^{12}	2.2×10^{11}	RT
Al	100	1×10^{13}	2.2×10^{11}	RT
Al	100	3×10^{13}	2.2×10^{11}	RT
Al	100	1×10^{14}	2.2×10^{11}	RT
Al	100	5×10^{14}	2.2×10^{11}	RT
Al	100	1×10^{15}	2.2×10^{11}	RT
Al	100	5×10^{14}	2.2×10^{11}	200
Al	100	5×10^{14}	2.2×10^{11}	400
Al	100	5×10^{14}	2.2×10^{11}	600
Al	100	5×10^{14}	2.2×10^{11}	800
Si	100	5×10^{14}	1.9×10^{10}	100
Si	100	5×10^{14}	2.2×10^{11}	100
Si	100	5×10^{14}	1.9×10^{12}	100
Si	100	5×10^{14}	2.3×10^{13}	100
Si	100	5×10^{14}	4.9×10^{13}	100

study the effect of the implantation temperature on the damage production. This set was implanted with 5×10^{14} cm^{-2} 100-keV Al ions and the implantation temperature was varied from RT to 800 °C. The ion flux for this set of samples was kept at 4×10^{11} cm^{-2} s^{-1}. The third set of samples was implanted with 100-keV Si ions. For this set, the ion fluence was 5×10^{14} cm^{-2} and the ion flux was varied from 1.9 $\times 10^{10}$ to 4.9×10^{13} cm^{-2} s^{-1}. The projected range of the implanted ions in all the samples was approximately 120 nm. For the first and second set, the samples were thin epitaxial layers (≈ 10 μm), weakly *n* type, grown by chemical vapor deposition on commercial bulk 4H–SiC. For the third set, the samples were Cree 4H–SiC *n*-type bulk wafers with a resistivity of 0.015 Ω m. (See Table I.)

B. Positron annihilation spectroscopy

Although the main damage occurs in the depth interval of 0–120 nm, i.e., up to the projected range, we expect to see point defects up to 1 μm due to channeling effects.[29] We therefore used a monoenergetic positron beam suitable for studying thin epitaxial layers. Monoenergetic positron beams are usually formed of positrons emitted from a radioactive β^+ source, e.g., ^{22}Na. After moderation the positrons are accelerated to the desired energy ($\approx 0-40$ keV). This enables the study of vacancy-type defects to a depth of a few micrometers. After implantation the positrons thermalize rapidly (thermalization time of <5 ps at RT) and thereafter diffuse in the lattice until they annihilate with electrons. Neutral and negative vacancy-type defects in the lattice act as positron traps. When a positron is trapped by such a defect its lifetime increases and the positron-electron momentum distribution narrows due to the reduced electron density.

The momentum of the annihilating positron-electron pair can be detected as Doppler broadening of the 511-keV annihilation line. The Doppler spectrum is influenced by the resolution of the detector. In our experiments we used a Ge detector with an energy resolution of 1.3 keV at 511 keV. The shape of the broadened annihilation line is usually described

by the parameters S and W. The low-momentum parameter S is the fraction of counts in the central part of the line and thus it describes mainly annihilation with low-momentum valence electrons. Correspondingly W is the high-momentum parameter obtained as the fraction of counts in the wing region of the annihilation line and it thus describes annihilation mainly with core electrons. Consequently, an increase (decrease) in the S (W) parameter indicates the presence of vacancy-type defects. The measured S (W) parameter is a superposition of the S (W) parameter of the bulk and the parameters of the vacancy-type defects in the sample. Hence, the measured S (W) is given by

$$S = \eta_B S_B + \sum \eta_{Di} S_{Di}, \tag{1}$$

$$W = \eta_B W_B + \sum \eta_{Di} W_{Di}. \tag{2}$$

In the above equations η_B is the fraction of positrons annihilating in the bulk state and η_{Di} is the fraction of positrons annihilating in the defect state i. S_B (W_B) and S_{Di} (W_{Di}) are the bulk and defect i S (W) parameters, respectively. If a sample contains only one type of defect the S-W plot of the measurement should form the segment of a line between the defect state and the bulk state. Large deviations from this line indicates that positrons are trapped by more than one type of defect, i.e., annihilate in more than two annihilation states. Near the surface, at low implantation energies, also the annihilation of the positrons at the surface has to be accounted for.

C. Ion-beam techniques

In order to study the crystalline quality of the implanted samples, Rutherford backscattering spectrometry in the channeling mode was employed. Channeled spectra along the $\langle 0001 \rangle$ direction were measured using 2.0- and 2.4-MeV He$^+$ beam from a tandem accelerator. The scattering chamber was equipped with a three-axis goniometer and sample control and data acquisition were computer controlled. The backscattering angle was 167° relative to the incident beam and Si solid-state detectors were used. Typically an ion charge less than 60 μC was accumulated during the alignment and recording of each channeling spectrum.

III. EXPERIMENTAL RESULTS

A. Rutherford backscattering spectrometry/channeling

Figure 1 shows the $\langle 0001 \rangle$-channeled RBS spectra from some selected samples. The dependence on ion fluence can be seen in Fig. 1(a) along with a random spectrum. The differences between the higher fluences are clearly visible, whereas the spectra cannot be distinguished from each other when the fluence is lower than 10^{13} cm^{-2}. At these ion fluences no significant crystalline damage is detected, i.e., the backscattering yield is close to that from the virgin crystal.

Figure 1(b) shows the results for the implantations done at elevated temperatures. A significant reduction in the backscattering yield can be seen already at 200 °C. When the implantation temperature is increased above 400 °C, the
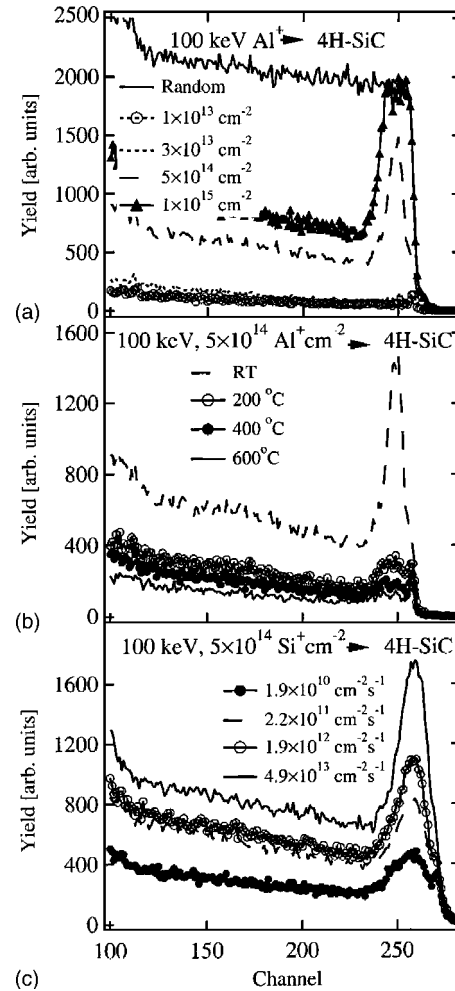

FIG. 1. (a) RBS channeling spectra of 4H–SiC implanted with varying fluences of 100-keV Al$^+$ ions. A random spectrum is also shown. (b) RBS channeling spectra of 4H–SiC implanted Al$^+$ (100 keV) ions at different temperatures. The ion fluence in all the implantations was 5×10^{14} cm^{-2}. (c) RBS channeling spectra of 4H–SiC implanted with varying fluxes of 5×10^{14} cm^{-2} 100-keV Si$^+$ ions

implantation-induced damage has diminished substantially and the crystal seems to recover almost completely during implantation.

The effect of the ion flux on the amount of displaced Si lattice atoms in the silicon-implanted samples is revealed in Fig. 1(c). As can be seen, the RBS yield in the channeled direction increases with increasing flux, showing more disorder in the crystal.

B. Positron annihilation spectroscopy

In Fig. 2 we show a set of S parameter versus positron implantation energy plots of each of the different sample types. Figure 2(a) shows the S parameter for the samples implanted with different fluences. Fig. 2(b) shows the S parameter after implantation at different temperatures, and Fig. 2(c) shows implantation with different fluxes. The results in Figs. 2(a) and 2(c) indicate that more vacancy-type defects (implantation damage) are formed at increasing fluence or flux. However, the result for implantation at elevated temperatures [Fig. 2(b)] shows an increasing S parameter in the projected range region with increasing implantation tempera-
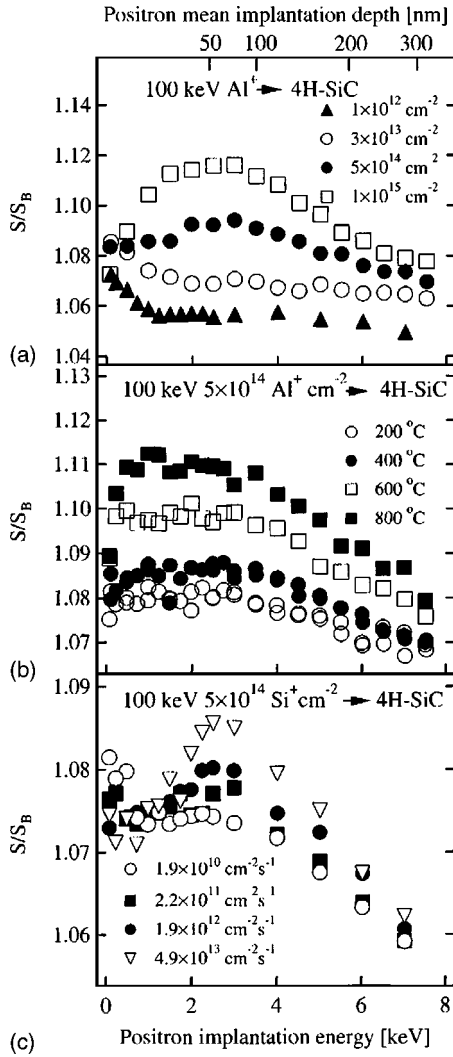
FIG. 2. The PAS Doppler parameter S as a function of positron implantation energy in the projected range region for (a) different fluences, (b) different implantation temperatures, and (c) different fluxes. Also indicated is the positron mean implantation depth.
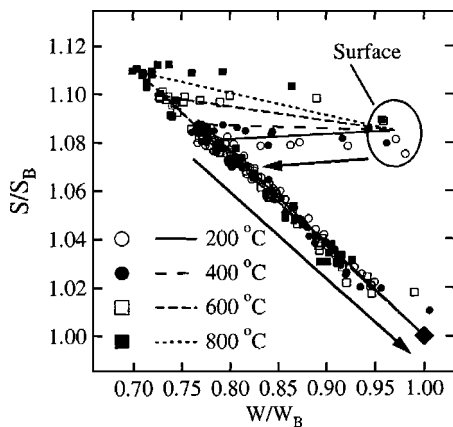

FIG. 4. Damage production as a function of ion fluence for 100-keV RT Al-implanted samples. (a) Normalized S parameter from the projected range region. (b) Normalized W parameter from the projected range region. Indicated in (a) and (b) are the characteristic S and W parameter levels for the t_1 and t_2 traps from Ref. 29. (c) Normalized RBS/channeling yield from the projected range region. Below the ion fluence of 10^{13} cm^{-2} the backscattering yield approaches the virgin crystal yield. The dashed lines are guides to the eye.

FIG. 3. S-W plot of 100-keV Al implantations into 4H–SiC at different temperatures. The arrows indicate increasing positron implantation energy and the lines are guides to the eye. Also indicated in the figures is the surface annihilation state and the bulk state (1.0, 1.0).
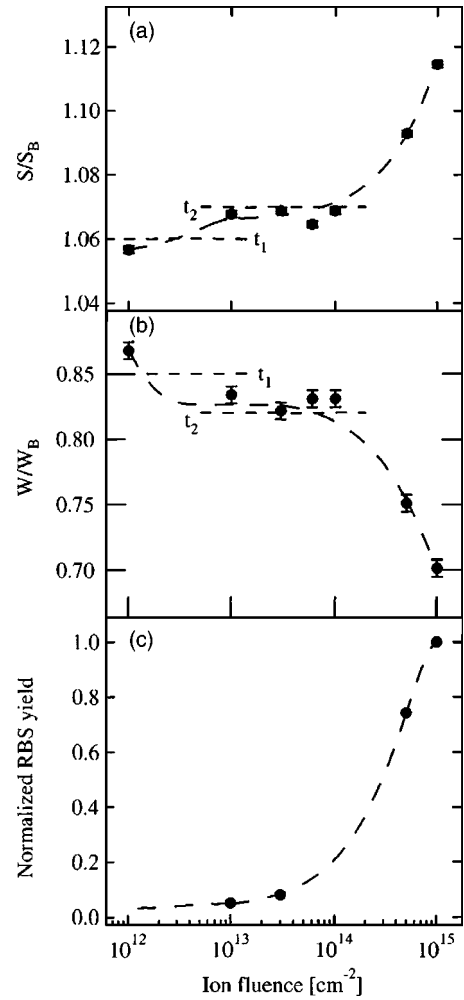
ture, indicating that either the concentration of the vacancy-type defects or the size of their open volume increases.

In order to clarify the effect seen in Fig. 2(b), the Doppler parameters are plotted in the (W,S) plane (Fig. 3). The measured (W,S) points for all samples fall on two lines, one line from the surface to the defect state in the projected range region ($1.5–3$ keV) and one from the defect state to the bulk state. The sharp shift from the surface–defect line to the defect–bulk line is an indication that the positron trapping in the projected range region is in saturation (all positron annihilate in vacancy-type defects) in all of the sample data depicted in Fig. 3. Thus, the turning point from the surface–defect line to the defect–bulk line is the characteristic S and W parameters for the dominant vacancy-type defect at each implantation temperature. Together with the fact that the S (W) parameter is increasing with increasing annealing temperature, this indicates that the size of the vacancy-type defect is increasing with increasing implantation temperature.

IV. DISCUSSION

A. Damage production as a function of ion fluence

Figure 4 shows the normalized PAS Doppler parameters and the RBS/channeling yield as a function of ion fluence for the 100-keV Al-implanted samples. The points shown in the figure have been extracted as averages from the original data for the projected range region. As expected the backscattering yield relative to the virgin crystal increases with increasing ion fluence [Fig. 4(c)], indicating more displaced Si atoms. Below 10^{13} cm^{-2} the backscattering signal approaches that of the virgin crystal and thus no damage is observed.

From the PAS results in Figs. 4(a) and 4(b) the following can be concluded: From 10^{12} to 10^{13} cm^{-2} the S (W) parameter increases (decreases) slowly, thereafter it stays approximately constant in the fluence interval of 10^{13}–10^{14} cm^{-2}. Above 10^{14} cm^{-2} the S (W) parameter increases (decreases) rapidly. The behavior of the PAS parameters thus differs from the RBS/channeling results. In Figs. 4(a) and 4(b) we have indicated the S and W parameter levels of the t_1 and t_2 positron traps determined in Ref. 29. These traps were tentatively identified[29] as a Si monovacancy V_{Si} (t_1) and a silicon carbon divacancy $V_C V_{Si}$ (t_2) by comparing to previous experimental[14,20] and theoretical results.[30,31]

The interpretation of Figs. 4(a) and 4(b) is the following: Below the ion fluence of 10^{13} cm^{-2} positrons are trapped and annihilated at mono- and divacancies. When the ion fluence reaches 10^{13} cm^{-2}, annihilation at divacancies dominate and the concentration of divacancies is high enough for saturation trapping, i.e., all positrons annihilate at divacancies. When the ion fluence is further increased, larger vacancy clusters can be formed, and above 10^{14} cm^{-2} the trapping of positrons to these larger open volume defects starts to dominate and the S (W) parameter begins to increase (decrease) rapidly. This interpretation is in agreement with the RBS/channeling results in Fig. 4(c), which measure the total amount of displaced Si atoms and not specific defects.

B. Damage production as a function of implantation temperature

The influence of the implantation temperature on the amount of damage is summarized in Fig. 5. The PAS Doppler parameters shown in Figs. 5(a) and 5(b) are extracted from the projected range region. All samples were implanted with an ion fluence of 5×10^{14} cm^{-2} and with the same ion flux. The points marked with an open circle represent samples that were implanted with Si. All the other points are from the Al-implanted samples. Since the atomic masses of Si and Al are very close, there should not be any significant differences in the damage production between these two kinds of ions. The implantation temperature was varied between RT and 800 °C.

From the RBS results in Fig. 5(c) it can be noted that the fraction of displaced atoms decreases rapidly with increasing implantation temperature. Already at an implantation temperature of 400 °C the crystal seems to recover almost completely during implantation. However, the PAS measurement indicates that the microscopic processes are more complicated. In the temperature interval from RT to 100 °C the
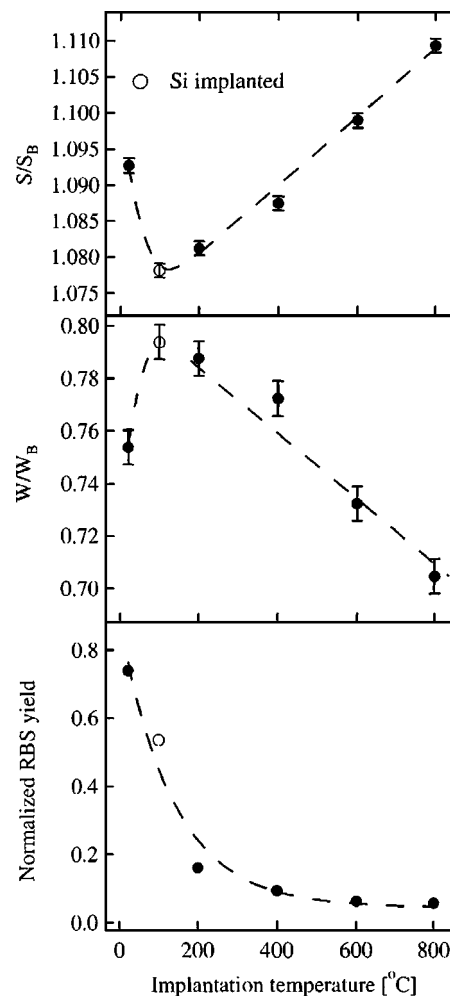

FIG. 5. Damage production as a function of implantation temperature. All the solid symbols have been implanted with 5×10^{14} cm^{-2} 100-keV Al ions with the same flux. The open symbol point has been implanted with 5×10^{14} cm^{-2} 100-keV Si ions with approximately the same flux as the Al implantations. Figures (a) and (b) show the normalized S and W parameters from the projected range region, respectively. Figure (c) shows the normalized RBS channeling yield from the projected range region. The dashed lines are guides to the eye.

S (W) parameter is decreasing (increasing). When the implantation temperature is increased above 100 °C the S parameter starts to increase, whereas the RBS minimum yield continues to decrease.

The decreasing S (increasing W) parameter below 100 °C, combined with the decreasing RBS minimum yield, is an indication that the concentration of the open volume defects in the samples is decreasing. Since the PAS S (W) parameter is clearly above (below) the value for the divacancy already at 100 °C which can also be clearly seen from the $W(S)$ plot in Fig. 3, we conclude that the increase (decrease) in the S (W) parameter above 100 °C is due to the formation of larger open volume defects, i.e., vacancy clustering. At 800 °C the S parameter value at the projected range (≈ 1.11) indicates that the vacancy clusters trapping positrons consist of more than five monovacancies.[32]

The vacancy clustering at such low temperatures indicates that the vacancies are mobile during the implantation process. This seems possibly to be in contradiction with cal-
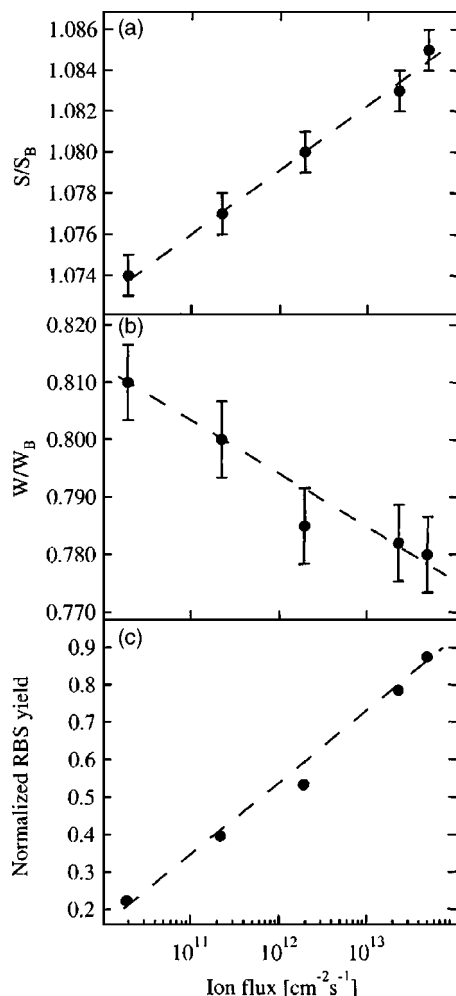
FIG. 6. Damage production as a function of ion flux for 5×10^{14} cm^{-2} 100-keV Si ion implantations. The implantations were done at a temperature of 100 °C. Figures (a) and (b) show the normalized PAS Doppler parameters S and W and Fig. (c) shows the corresponding RBS channeling yield from the projected range region. The dashed lines are guides to the eye.

culated migration barriers for vacancies in SiC and with experimental diffusion studies, which usually require much higher annealing temperatures.[33–36] However, it must be noted that the theoretical calculations and diffusion studies are done assuming thermal equilibrium, whereas in the case of implantation at high temperatures the crystal is far from being in thermal equilibrium and in addition, ionization-enhanced defect migration may also appear.

C. Damage production as a function of ion flux

In Fig. 6 we show the S and W parameters from the PAS measurements (projected range region) and the normalized RBS yield for samples implanted with 5×10^{14} cm^{-2} 100-keV Si ions at 100 °C as a function of ion flux. As can be seen from the RBS/channeling signal [Fig. 6(c)] the differences between the lowest and highest ion fluences are significant. The crystal structure changes from an ordered structure to an almost amorphous state when the ion flux is increased from 10^{10} to 10^{13} cm^{-2} s^{-1}.[9]

The changes in the PAS Doppler parameters are not as dramatic. The increase in the normalized S parameter is

roughly 1% in this flux interval. The S parameter value is slightly above the t_2 level, indicating that no significant concentration of larger open volume defects is formed during the implantation.

The RBS/channeling and PAS results can be understood by noting that the PAS S and W parameters are very close to the divacancy level t_2. It is therefore difficult to estimate the concentration of the vacancy-type defects in the samples since the positron trapping is in saturation. A small change in the S (W) parameter can reflect a large change in the concentration of vacancy defects. In general, it can be concluded that since the changes in the Doppler parameters are small, the average open volume in the implanted samples is approximately constant and close to that of a divacancy.

V. CONCLUSIONS

In this study we have reported on damage production in ion-implanted 4H–SiC investigated with ion-beam methods and positron annihilation spectroscopy. The amount of damage in the ion projected range region was studied as a function of ion fluence, ion flux, and implantation temperature. As expected the number of displaced silicon atoms is found by RBS channeling measurements to increase rapidly with increasing ion fluence. The PAS measurements show that both mono- and divacancies exist at fluences below 1 $\times 10^{13}$ cm^{-2}. In the fluence interval of 1×10^{13} cm^{-2}–1 $\times 10^{14}$ cm^{-2} all positrons annihilate at divacancies.

RBS channeling measurements show that the fraction of displaced silicon atoms decreases rapidly when the implantation temperature is increased to 200 °C, and above 400 °C the RBS minimum yield approaches that of the virgin crystal. The PAS results show that two different microscopic processes take place depending on the implantation temperature. Below 100 °C the PAS Doppler parameters behave as the RBS minimum yield, indicating vacancy recovery. However, above 100 °C the vacancy-type defects in the implanted samples start to agglomerate into large vacancy clusters.

For samples implanted at different ion fluxes but with the same fluence, the RBS channeling yield shows a dramatic change from an ordered crystal into an almost amorphous state when the ion flux is increased from 10^{10} to 10^{13} cm^{-2} s^{-1}. The associated changes in the PAS Doppler parameters are observed but they show that divacancies remain as the dominant defects at all fluxes. The clustering of vacancies seems to result from the increased ion-implantation fluence and temperature, but to much smaller extent from the increased flux.

ACKNOWLEDGMENTS

[1] M. V. Rao, P. Griffiths, O. W. Holland, G. Kelner, J. J. A. Freitas, D. S. Simons, P. H. Chi, and M. Ghezzo, J. Appl. Phys. **77**, 2479 (1995).
[2] T. Kimoto, A. Itoh, N. Inoue, O. Takamura, T. Yamamoto, T. Nakajima, and H. Matsunami, Mater. Sci. Forum **264–268**, 675 (1998).
[3] T. Troffer, M. Schadt, T. Frank, H. Itoh, G. Pensl, J. Heindl, H. P. Strunk,

and M. Maier, *Silicon Carbide: A Review of Fundamental Questions and Applications to Current Device Technology* (Akademie, Berlin, 1997), p. 277.

[4]E. Wendler, A. Heft, and W. Wesch, Nucl. Instrum. Methods Phys. Res. B **141**, 105 (1998).

[5]A. Mattausch, M. Bockstedte, and O. Pankratov, Mater. Sci. Forum **353–356**, 323 (2001).

[6]M. Bockstedte, M. Heid, A. Mattausch, and O. Pankratov, Mater. Sci. Forum **389–393**, 471 (2002).

[7]T. Kimoto, N. Inoue, and H. Matsunami, Phys. Status Solidi A **162**, 263 (1997).

[8]J. Slotte, K. Saarinen, A. Y. Kuznetsov, and A. Hallén, Physica B **308–310**, 664 (2001).

[9]A. Y. Kuznetsov, J. Wong-Leung, A. Hallén, C. Jagadish, and B. G. Svensson, J. Appl. Phys. **94**, 7112 (2003).

[10]M. Posselt, L. Bischoff, J. Teichert, and A. Ster, J. Appl. Phys. **93**, 1004 (2003).

[11]K. Saarinen, P. Hautojärvi, and C. Corbel, *Identification of Defects in Semiconductors*, edited by M. Stavola (Academic, New York, 1998).

[12]R. Krause-Rehberg and H. S. Leipner, *Positron Annihilation in Semiconductors* (Springer, Heidelberg, 1999).

[13]M. A. Müller, A. A. Rempel, K. Reichle, W. Sprengel, J. Major, and H. E. Schaefer, Mater. Sci. Forum **363–365**, 70 (2001).

[14]S. Arpiainen, K. Saarinen, P. Hautojärvi, L. Henry, M.-F. Barthe, and C. Corbel, Phys. Rev. B **66**, 075206 (2002).

[15]G. Brauer *et al.*, Phys. Rev. B **54**, 3084 (1996).

[16]A. I. Girka, A. D. Mokrushin, E. N. Mokhov, S. V. Svirida, and A. V. Shishkin, Mater. Sci. Forum **105–110**, 1021 (1992).

[17]A. Uedono *et al.*, Jpn. J. Appl. Phys., Part 1 **36**, 6650 (1997).

[18]A. Uedono *et al.*, Jpn. J. Appl. Phys., Part 1 **37**, 2422 (1998).

[19]A. Uedono *et al.*, J. Appl. Phys. **87**, 4119 (2000).

[20]G. Brauer, W. Anwand, P. G. Coleman, J. Störmer, F. Plazaola, J. M. Campillo, Y. Pacaud, and W. Skorupa, J. Phys.: Condens. Matter **10**, 1147 (1998).

[21]H. Itoh *et al.*, Appl. Phys. A: Mater. Sci. Process. **65**, 315 (1997).

[22]H. Wirth, W. Anwand, G. Brauer, M. Voelskow, D. Panknin, and W. Skorupa, Mater. Sci. Forum **264–268**, 729 (1998).

[23]C. J. McHargue and J. M. Williams, Nucl. Instrum. Methods Phys. Res. B **80–81**, 889 (1993).

[24]W. Wesch, A. Heft, J. Heindl, H. P. Strunk, T. Bachmann, E. Glaser, and E. Wendler, Nucl. Instrum. Methods Phys. Res. B **106**, 339 (1995).

[25]W. J. Weber, W. Jiang, Y. Zhang, and A. Hallén, Nucl. Instrum. Methods Phys. Res. B **191**, 514 (2002).

[26]Y. Zhang, W. J. Weber, W. Jiang, C. M. Wang, A. Hallén, and G. Possnert, J. Appl. Phys. **93**, 1954 (2003).

[27]Y. Zhang, W. J. Weber, W. Jiang, A. Hallén, and G. Possnert, J. Appl. Phys. **91**, 6388 (2002).

[28]M. S. Janson, J. Slotte, A. Y. Kuznetsov, K. Saarinen, and A. Hallèn, J. Appl. Phys. **95**, 57 (2004).

[29]M. S. Janson, J. Slotte, A. Y. Kuznetsov, K. Saarinen, and A. Hallèn, Mater. Sci. Forum **433–436**, 641 (2003).

[30]G. Brauer *et al.*, Phys. Rev. B **54**, 2512 (1996).

[31]T. E. M. Staab, L. M. Torpo, M. J. Puska, and R. M. Nieminen, Mater. Sci. Forum **353**, 533 (2001).

[32]M. Hakala, M. J. Puska, and R. M. Nieminen, Phys. Rev. B **57**, 7621 (1998).

[33]M. Bockstedte, A. Mattausch, and O. Pankratov, Phys. Rev. B **68**, 205201 (2003).

[34]L. Torpo, M. Marlo, T. E. M. Staab, and R. M. Nieminen, J. Phys.: Condens. Matter **13**, 6203 (2001).

[35]M. H. Hon, R. F. Davis, and D. E. Newbury, J. Mater. Sci. **15**, 2073 (1980).

[36]M. K. Linnarson, M. S. Janson, J. Zhang, E. Janzén, and B. G. Svensson, J. Appl. Phys. **95**, 8469 (2004).